Investigation Of Higher-Harmonic Wave Forces And Ringing using CFD Simulations

Arun Kamath[1]*, Csaba Pakozdi[2] and Hans Bihs[1]

[1]Department of Civil and Environmental Engineering, Norwegian University of Science and Technology (NTNU), 7491 Trondheim, Norway
[2]SINTEF Ocean, Trondheim, Norway

Presented at *37th International Conference on Ocean, Offshore and Arctic Engineering, OMAE2018, Madrid, Spain* 17-22 June 2018.

Abstract

Typical offshore structures are designed as tension-leg platforms or gravity based structures with cylindrical substructures. The interaction of waves with the vertical cylinders in high sea states can result in a resonant response called ringing. Here, the frequency of the structural response is close to the natural frequency of the structure itself and leads to large amplitude motions. This is a case of extreme wave loading in high sea states. This understanding of higher-order wave forces in extreme sea states is an essential parameter for obtaining a safe, reliable and economical design of an offshore structure. The study of such higher-order effects needs detailed near-field modelling of the wave-structure interaction and the associated flow phenomena. In such cases, a Computational Fluid Dynamics (CFD) model that can accurately represent the free surface and further the wave-structure interaction problem can provide important insights into the wave hydrodynamics and the structural response. In this paper, the open source CFD model REEF3D is used to simulate wave interaction with a vertical cylinder and the wave forces on the cylinder are calculated. The harmonic components of the wave force are analysed. The model employs higher-order discretisation schemes such as a fifth-order WENO scheme for convection discretisation and a third-order Runge-Kutta scheme for time advancement on a staggered Cartesian grid. The level set method is used to obtain the free surface, providing a sharp interface between air and water. The relaxation method is used to generate and absorb the waves at the two ends of the numerical wave tank. This method provides good quality wave generation and also the wave reflected from the cylinder are absorbed at the wave generation zone. In this way, the generated waves are not affected by the wave interaction process in the numerical wave tank. This is very essential in the studies of higher-order wave interaction problems which are very sensitive to the incident wave characteristics. The numerical results are compared to experimental results for higher-order forces on a vertical cylinder to validate the numerical model.

*Corresponding author, arun.kamath@ntnu.no

Keywords: ringing; wave forces; breaking wave; CFD; REEF3D

1 Introduction

Offshore structures such as tension-leg platforms, gravity based structures with cylindrical substructures and offshore wind turbine substructures are exposed to harsh wave climates. One of the important phenomena that the offshore structures can be susceptible to is the phenomenon of ringing. Here, in severe sea states, the structure responds at frequencies that are higher than the incident wave frequency. This higher-order response phenomenon can be identified through investigation of the wave force regime on a cylinder under different wave conditions and from the presence of the higher-order components in the force regime. The presence of higher-order components in the wave forces can lead to resonance with the natural frequency of the structure, leading to ringing of the structure.

Several authors have studied the phenomenon of ringing through mathematical Faltinsen et al. (1995) Malenica and Molin (1995) and experimental investigations Chaplin et al. (1997) Grue and Huseby (2002). Current literature reports that while the higher-order resonance phenomenon of ringing is readily observed in the cases involving wave impact such as wave breaking on a structure Welch et al. (1999) and in the case of focussed wave interaction with structures, it is also seen in the case of non-breaking waves of moderate steepness. Thus, this phenomenon os of great interest for a safe and economical design of an offshore structure.

With current advances in computing power, several complex free surface problems can be investigated using computational fluid dynamics (CFD) modeling. Three-dimensional numerical modeling can provide new insights into the wave hydrodynamics and provide more knowledge regarding the flow phenomenon. The study of higher-order effects can be carried out through a range of simulations for different wave types, wave conditions and configurations of the structure to determine the wave force regime on the structure and assess its susceptibility to higher-order resonant effects such as ringing. The authors are not aware of such numerical analysis using results from a 3D CFD-based numerical model for plunging breaking waves on a cylinder.

In this paper, the interaction of focussed waves, non-breaking regular waves in deep water and regular waves undergoing depth induced breaking on a vertical cylinder is investigated using the open-source CFD model REEF3D Bihs et al. (2016*b*) which has been apllied to several coastal and marine engineering problems such as wave near-trapping in cylinder groups Kamath et al. (2016*b*), kinematics of breaking waves Alagan Chella et al. (2016), breaking wave forces Kamath et al. (2016*a*) Alagan Chella et al. (2017) and floating bodies in waves Bihs and Kamath (2017). The calculated wave forces are compared to experimental data to validate the model. The simulations using focussed waves are compared to experimental data presented by Chen et al. Chen et al. (2014). The simulation with regular non-breaking waves in deep water is compared to data from the model test carried out at MARINTEK, Trondheim, Norway Stansberg (1997). Finally, the breaking wave forces on a vertical cylinder due to regular waves undergoing depth induced breaking after propagating over a $1:10$ slope are evaluated. The wave forces in all the cases are also analyzed to identify the higher-order contributions in the total wave force.

2 Numerical Model

The incompressible Reynolds-Averaged Navier-Stokes (RANS) equations are used to solve the fluid flow problem:

$$\frac{\partial u_i}{\partial x_i} = 0 \tag{1}$$

$$\frac{\partial u_i}{\partial t} + u_j \frac{\partial u_i}{\partial x_j} = -\frac{1}{\rho}\frac{\partial p}{\partial x_i} + \frac{\partial}{\partial x_j}\left[(\nu + \nu_t)\left(\frac{\partial u_i}{\partial x_j} + \frac{\partial u_j}{\partial x_i}\right)\right] + g_i \tag{2}$$

where u is the time averaged velocity, ρ is the density of water, p is the pressure, ν is the kinematic viscosity, ν_t is the eddy viscosity, t is time and g is the acceleration due to gravity. Chorin's projection method Chorin (1968) is used for the pressure treatment. The high performance solver library HYPRE Center for Applied Scientific Computing (2006) is employed to solve the Poisson pressure equation using the PFMG-preconditioned BiCGStab algorithm Ashby and Flagout (1996).

Turbulence modelling is carried out based on Durbin's modification Durbin (2004) of the two equation k-ω model proposed by Wilcox Wilcox (1994). Eddy viscosity, ν_t, is bounded to avoid unphysical overproduction of turbulence in strained flow as shown by DurbinDurbin (2009). The large difference in density of air and water in a two-phase model leads to an overproduction of turbulence at the interface due to large strain. For this reason, free surface turbulence damping is introduced around the interface based on the studies by Naot and Rodi (1982).

The fifth-order conservative finite difference Weighted Essentially Non-Oscillatory (WENO) scheme proposed by Jiang et al. Jiang and Shu (1996) is used for the discretization of convective terms for the velocity u_i, the level set function ϕ, turbulent kinetic energy k and the specific turbulent dissipation rate ω. A TVD third-order Runge-Kutta explicit time scheme developed by Harten Harten (1983) is employed for time discretization in the model. It is a three-step scheme and involves the calculation of the spatial derivatives three times per time step. This scheme is used for the time advancement of the level set function and the reinitialisation equation.

A Cartesian grid is used in the numerical model for spatial discretization. The Immersed Boundary Method (IBM) Peskin (1972) is used to incorporate the boundary conditions for complex geometries. The free surface is obtained using the level set method where the zero level set of a signed distance function, $\phi(\vec{x}, t)$ is used to represent the interface between air and water. Moving away from the interface, the level set function gives the closest distance of the point from the interface. The sign of the function represents the two fluids across the interface. The level set function is reinitialised after every iteration using a partial differential equation (PDE) based reinitialisation procedure presented by Sussman et al.Sussman et al. (1994) to retain its signed distance property after convection.

Further details regarding the model can be found in Bihs et al. Bihs et al. (2016*b*) and details regarding focussed wave generation in REEF3D can be found in Bihs et al. (2016*a*).

3 Results

3.1 Comparison with wave forces due to focused waves

In this section, the interaction of focussed waves with a vertical cylinder is investigated using REEF3D and the numerical results are compared to experimental results to validate the model. The wave forces are analysed to obtain the higher-order components. The numerical wave tank is 10 m long, 2 m wide and 1 m high with a water depth of $d = 0.505$ m. Three cases are simulated following the results presented by Chen et al. (2014). Focussed waves of peak period $T_p = 1.22$ s and focus height $H = 0.14$ m, peak period $T_p = 1.63$ s and focus heights 0.12 m, 0.24 m are simulated. The results for the wave forces are presented in Figs.(1), (2) and (3). The numerical results and the experimental data for the wave forces due to the focussed wave with peak period $T_p = 1.22$ s and focus height 0.14 m agree very well in Fig.(1a). The amplitude spectrum of the wave forces does not show any significant peaks away from the incident frequency of 0.82 Hz, just like in the experimental data. In this case, the wave forces do not have higher-order components and thus ringing due to the wave loading is not expected.

In the next case, with $T_p = 1.63$ s and $H = 0.12$ m the numerical results are compared with the experimental data in Fig.(2a) and a good agreement is found between the results. The amplitude spectrum of the wave forces shows a small peak close to the second harmonic $f_2 = 1.20$ Hz of the incident peak wave frequency $f_p = 0.6$ Hz. The amplitude of the peak at f_2 is about 15% of the peak at the incident frequency. Similarly, a simulation is carried out with a steeper wave with $T_p = 1.63$ s and $H = 0.24$ m and the results for the wave forces are presented in Fig.(3a). The plot of wave force over time shows some asymmetry due to the steepness of the incident wave. The amplitude spectrum of the wave force shows a peak at the second harmonic $f_2 = 1.20$ Hz and the magnitude of the peak in this case is about 21% of the peak at the incident frequency.

It is seen from the cases presented above that higher-order components in the wave force exist for incident waves with certain conditions of steepness and peak period and that the numerical model is able to calculate the higher-order forces due to focussed waves satisfactorily.

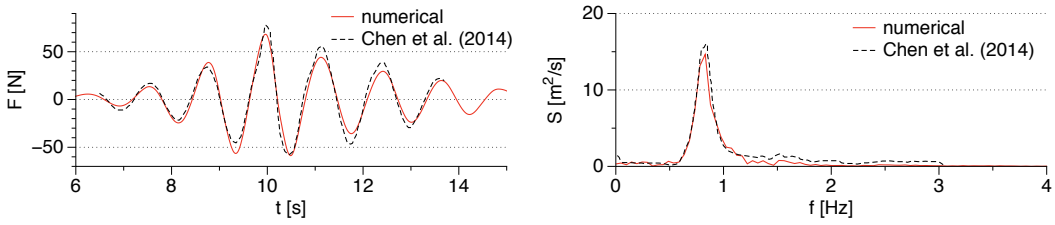

(a) wave force on the cylinder

(b) amplitude spectrum of the wave force

Figure 1: Wave forces on a cylinder due to focussed wave of height $H = 0.14$ m and peak period $T_p = 1.22$ s

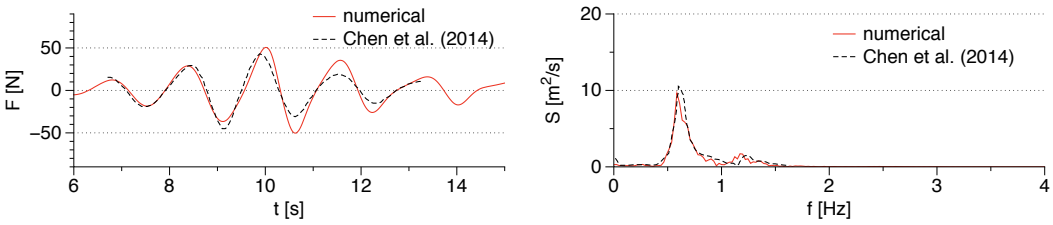

(a) wave force on the cylinder (b) amplitude spectrum of the wave force

Figure 2: Wave forces on a cylinder due to focussed wave of height $H = 0.12$ m and peak period $T_p = 1.63$ s

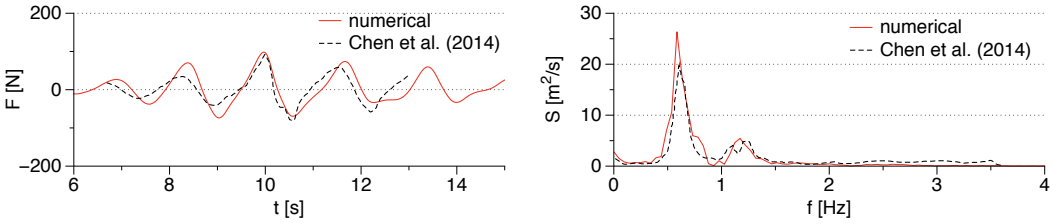

(a) wave force on the cylinder (b) amplitude spectrum of the wave force

Figure 3: Wave forces on a cylinder due to focussed wave of height $H = 0.24$ m and peak period $T_p = 1.63$ s

Comparison with model test of a truncated cylinder

The phenomenon of ringing is then analysed for deep water conditions with a truncated cylinder. The data from the experiments carried out at MARINTEK, Trondheim, Norway Stansberg (1997) are used for the comparison of the numerical results. In this case, a numerical wave tank 15 m long, 3 m wide and 7 m high with a water depth of $d = 5.0$ m is used. The cylinder has a diameter $D = 0.625$ m and regular waves of height $H = 0.440$ m and period $T = 1.73$ s are generated. The cylinder is truncated 1.50 m above the bottom of the tank. The numerically calculated wave forces on the cylinder are compared to the experimental measurements in Fig.(4a). The amplitude spectrum of the wave forces are compared in Fig.(4b). The numerical results match the results from the model test well. The highest peak is seen close to the incident wave frequency of $f = 0.58$ Hz. higher-order components are identified from the smaller peaks seen in the amplitude spectrum close to the third harmonic $f_3 = 1.73$ Hz. Thus, the numerical model is able to calculate the higher-order components involved in the wave interaction of regular waves with a vertical cylinder satisfactorily.
The interaction of the regular wave train with the truncated vertical cylinder is presented in Fig.(4). The circular waves due to the diffraction from the preceding wave trough is seen in Fig.(5a), while the next wave crest approaches the cylinder in Fig.(5b). Figure (5c) shows the wave crest interacting with the diffracted wave while being incident on the cylinder. The separation of the wavefront around the cylinder and runup on the front surface of the cylinder is seen in Fig.(5d). The separated wavefront meets behind the cylinder and the formation of semi-circular waves is seen as the wave crest propagates downstream of the cylinder in

Figs.(5e) and (5f).

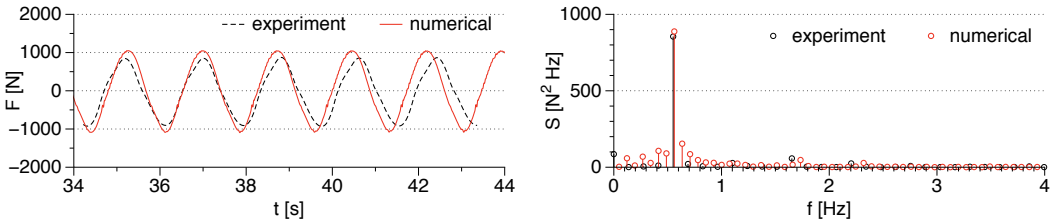

(a) wave force on the cylinder

(b) amplitude spectrum of the wave force

Figure 4: Comparison of numerical results with experimental data for wave forces and the amplitude spectrum of the wave forces on a truncated cylinder of $D = 0.625$ m in a water depth of $d = 5.0$ m due to incident waves of height $H = 0.440$ m and period $T = 1.73$ s

Ringing due to breaking wave impact

The impact of breaking waves on a cylinder leads to additional large response from the cylinder due to the impulsive nature of the breaking wave forces. The evaluation of the breaking wave forces and identification of the higher-order forces can provide important information regarding the response of the structure. In this section, breaking wave forces on a vertical cylinder is evaluated and the higher-order components in the calculated wave force are identified. A numerical wave tank 54 m long, 5 m wide and 7 m high with a water depth of $d = 3.80$ m is used. A 23 m long $1 : 10$ slope is placed in the tank to obtain depth-induced breaking of the incident regular waves. At the crest of the slope, a flat bed is placed with a height of 2.30 m from the bottom of the tank. The water depth over the flat bed is 1.50 m. A cylinder of diameter 0.7 m is placed at the crest of the slope with its axis at 44.0 m. Further details about the numerical setup and validation of the numerical model can be obtained from Kamath et al. Kamath et al. (2016*a*). Regular waves of period $T = 4.0$ s and height $H = 1.30$ m are generated in the wave tank. The breaking point of the wave is identified to be 43.65 m. The cylinder is placed with its axis at 46.35 m. In this configuration, the overturning wave crest impacts the cylinder just below the wave crest level. According to previous works Irschik et al. (2004) Kamath et al. (2016*a*), the cylinder experiences the maximum wave forces in this configuration for a given wave height and wave breaking point.

The calculated breaking wave forces on the cylinder are presented in Fig.(6a). The impulsive nature of the breaking wave impact is seen in the figure with sharp peaks in the force vs. time plot in the figure. The amplitude spectrum of the calculated wave forces are presented in Fig.(6b). Two peaks with similar amplitudes are seen in the frequency spectrum at the incident wave frequency $f = 0.25$ Hz and the second harmonic $f_2 = 0.5$ Hz. In addition, significant peaks are seen at the third, fourth, fifth and sixth harmonics at 1.0, 1.25, 1.50 and 1.75 Hz respectively. This shows that the wave forces on a cylinder due to breaking wave impact consists of several higher-order components. The numerical model is able to account for the total wave force on the cylinder considering the higher-order components and the results can be used to determine the response of the cylinder.

The interaction of the breaking wave with the cylinder is presented in Fig.(6).

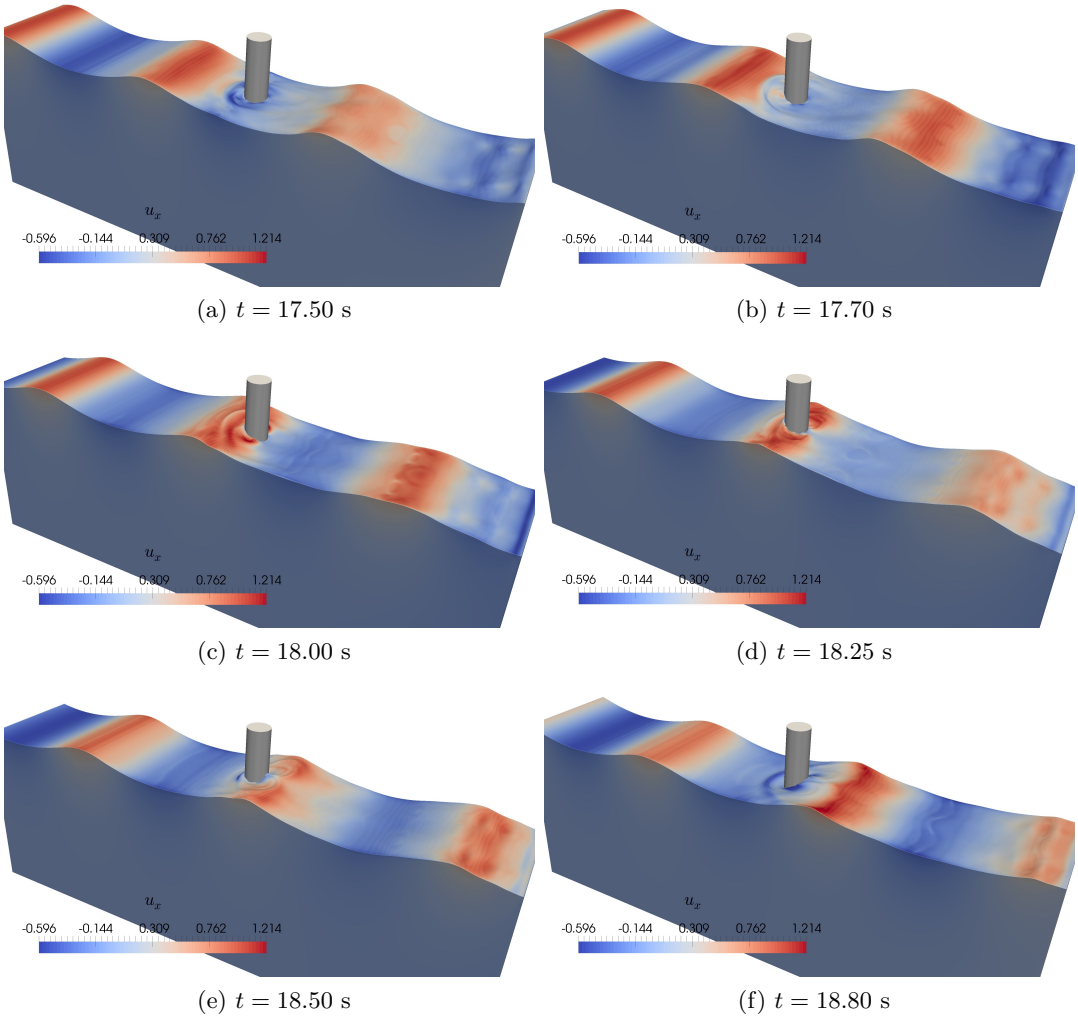

(a) $t = 17.50$ s (b) $t = 17.70$ s

(c) $t = 18.00$ s (d) $t = 18.25$ s

(e) $t = 18.50$ s (f) $t = 18.80$ s

Figure 5: Wave interaction with a truncated cylinder with $D = 0.625$ m in a numerical wave tank with water depth $d = 5.0$ m exposed to regular waves of height $H = 0.440$ m and period $T = 1.73$ s

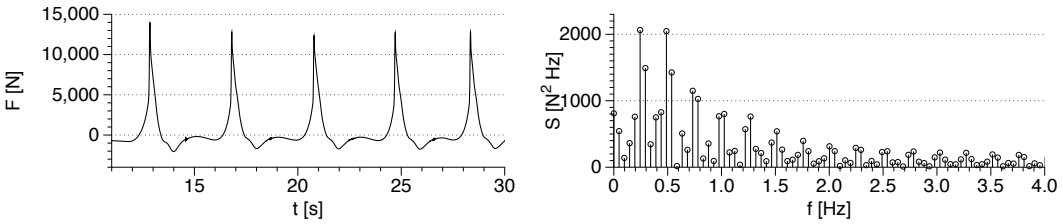

(a) wave force on the cylinder (b) amplitude spectrum of the wave force

Figure 6: Breaking wave forces and the amplitude spectrum of the wave forces on a vertcal cylinder due to breaking waves with an incident wave height of $H = 1.60$ m

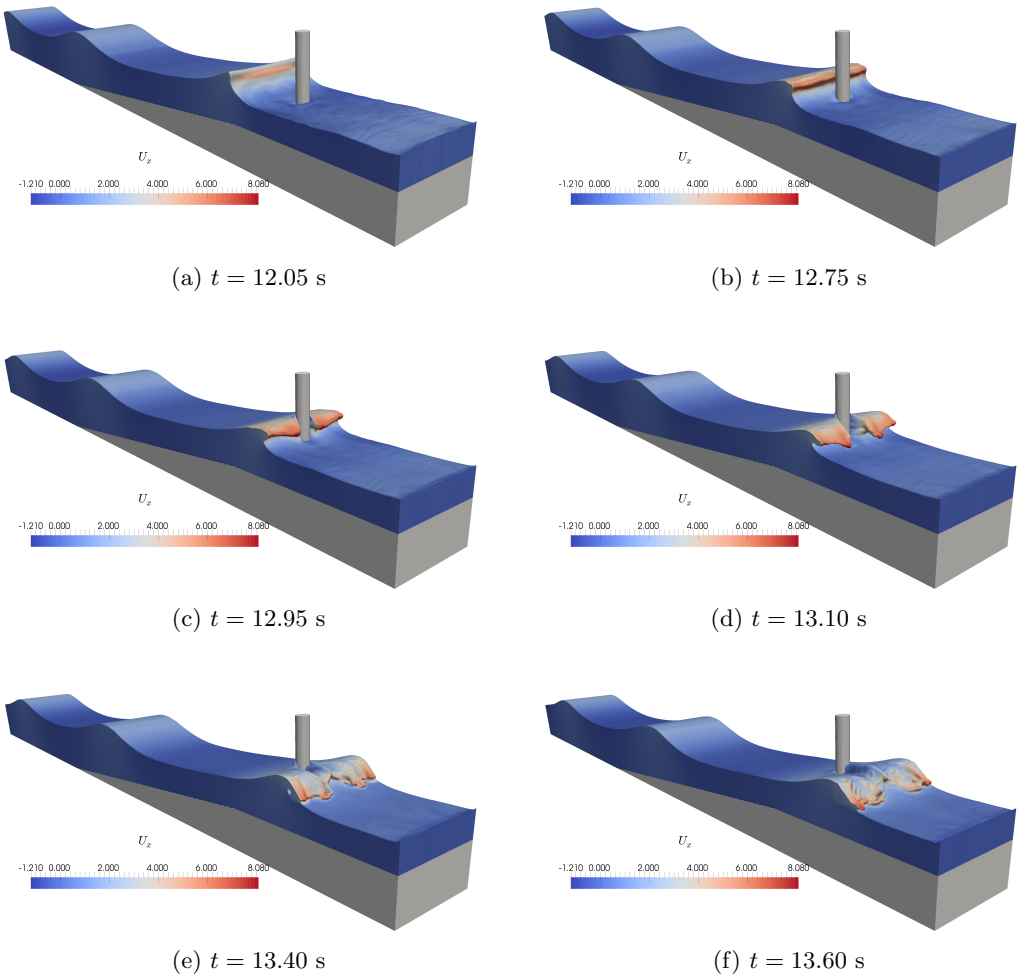

(a) $t = 12.05$ s

(b) $t = 12.75$ s

(c) $t = 12.95$ s

(d) $t = 13.10$ s

(e) $t = 13.40$ s

(f) $t = 13.60$ s

Figure 7: Breaking wave interaction with a vertical cylinder with $D = 0.70$ m in a numerical wave tank exposed to regular waves of height $H = 1.60$ m and period $T = 4.0$ s, placed on a flat bed at the crest of a 23 m long $1 : 10$ slope with a water depth of 1.50 m on the flat bed

4 Conclusions

The open-source CFD model REEF3D is used in this study to evaluate the wave forces on a vertical cylinder due to focussed waves, regular non-breaking waves and regular breaking waves. The numerical results are compared to experimental measurements in the case of focussed waves and non-breaking regular waves. A good agreement is seen between the numerical and experimental data for both the wave forces and the amplitude spectra to obtain the higher-order components.

In the case of the focussed waves, the higher-order components are seen for waves with focussed height of 0.12 m and 0.24 m produced using a spectrum with peak period of $T_p = 1.63$ s whereas they are not seen for focussed waves of height $H = 0.14$ m produced using a spectrum with peak period $T_p = 1.22$ m. The contribution of the higher-order forces is also higher for larger wave heights. The amplitude spectrum shows peaks at the second harmonic that are 15% and 21% of the peak obtained at the fundamental frequency for $H = 0.12$ m and $H = 0.24$ m respectively.

The breaking wave impact on a vertical cylinder is presented with the cylinder configured in a manner that the wave forces are maximum for the given wave period and water depth. The amplitude spectrum of the wave forces shows two similar peaks at the incident frequency and at the second harmonic. Further, significant peaks are seen up to the sixth harmonic of the incident wave frequency.

The forces evaluated by REEF3D for different wave conditions such as focussed waves, regular non-breaking waves and regular breaking waves is presented. The calculated wave forces and the amplitude spectrum of the wave forces are compared with experimental data for focussed waves and regular non-breaking waves in deep water. The model is seen to perform well with good agreement to experimental data. Further studies can be carried out by analysing the wave forces in different segments along the water depth and calculate the different hydrodynamic coefficients.

Acknowledgements

This research was supported in part with computational resources at NTNU provided by The Norwegian Metacenter for Computational Sciences (NOTUR, http://www.notur.no) under project no. NN2620K.

References

Alagan Chella, M., Bihs, H., Myrhaug, D. and Muskulus, M. (2016). Hydrodynamic characteristics and geometric properties of plunging and spilling breakers over impermeable slopes. *Ocean Modelling, Virtual Special Issue: Ocean Surface Waves*, **103**, 53–72.

Alagan Chella, M., Bihs, H., Myrhaug, D. and Muskulus, M. (2017). Breaking solitary waves and breaking wave forces on a vertically mounted slender cylinder over an impermeable sloping seabed. *Journal of Ocean Engineering and Marine Energy*, **3**(1), 1–19.

Ashby, S.F. and Flagout, R.D. (1996). A parallel mulitgrid preconditioned conjugate gradient algorithm for groundwater flow simulations. *Nuclear Science and Engineering*, **124**(1), 145–159.

Bihs, H., Alagan Chella, M., Kamath, A. and Arnsten, Ø.A. (2016*a*). Wave-structure interaction of focussed waves with REEF3D. In: *ASME 2016 35th International Conference on Ocean, Offshore and Arctic Engineering*, V002T08A027–V002T08A027.

Bihs, H. and Kamath, A. (2017). A combined level set/ghost cell immersed boundary representation for floating body simulations. *International Journal for Numerical Methods in Fluids*, **83**(12), 905–916.

Bihs, H., Kamath, A., Alagan Chella, M., Aggarwal, A. and Arntsen, Ø.A. (2016*b*). A new level set numerical wave tank with improved density interpolation for complex wave hydrodynamics. *Computers & Fluids*, **140**, 191–208.

Center for Applied Scientific Computing (2006). *HYPRE high performance preconditioners - User's Manual*. Lawrence Livermore National Laboratory.

Chaplin, J., Rainey, R. and Yemm, R. (1997). Ringing of a vertical cylinder in waves. *Journal of Fluid Mechanics*, **350**, 119–147.

Chen, L.F., Zang, J., Hillis, A.J., Morgan, G.C.J. and Plummer, A.R. (2014). Numerical investigation of wave–structure interaction using OpenFOAM. *Ocean Engineering*, **88**, 91–109.

Chorin, A. (1968). Numerical solution of the Navier-Stokes equations. *Mathematics of Computation*, **22**, 745–762.

Durbin, P.A. (2004). Turbulence closure models for computational fluid dynamics.

Durbin, P.A. (2009). Limiters and wall treatments in applied turbulence modeling. *Fluid Dynamics Research*, **41**, 1–18.

Faltinsen, O.M., Newman, J.N. and Vinje, T. (1995). Nonlinear wave loads on a slender vertical cylinder. *Journal of Fluid Mechanics*, **289**, 179–198.

Grue, J. and Huseby, M. (2002). Higher-harmonic wave forces and ringing of vertical cylinders. *Applied Ocean Research*, **24**, 203–214.

Harten, A. (1983). High resolution schemes for hyperbolic conservation laws. *Journal of Computational Physics*, **49**, 357–393.

Irschik, K., Sparboom, U. and Oumeraci, H. (2004). Breaking wave loads on a slender pile in shallow water. In: *Proc. 29th International Conference on Coastal Engineering, Lisbon, Portugal*.

Jiang, G.S. and Shu, C.W. (1996). Efficient implementation of weighted ENO schemes. *Journal of Computational Physics*, **126**, 202–228.

Kamath, A., Alagan Chella, M., Bihs, H. and Arntsen, Ø.A. (2016*a*). Breaking wave interaction with a vertical cylinder and the effect of breaker location. *Ocean Engineering*, **128**, 105–115.

Kamath, A., Bihs, H., Alagan Chella, M. and Arntsen, Ø.A. (2016*b*). Upstream-cylinder and downstream-cylinder influence on the hydrodynamics of a four-cylinder group. *Journal of Waterway, Port, Coastal, and Ocean Engineering*, **142**(4), 04016002. doi: 10.1061/(ASCE)WW.1943-5460.0000339.

Malenica, S. and Molin, B. (1995). Third-harmonic wave diffraction by a vertical cylinder. *Journal of Fluid Mechanics*, **302**, 203–229.

Naot, D. and Rodi, W. (1982). Calculation of secondary currents in channel flow. *Journal of the Hydraulic Division, ASCE*, **108**(8), 948–968.

Peskin, C.S. (1972). Flow patterns around the heart valves. *Journal of Computational Physics*, **10**, 252–271.

Stansberg, C.T. (1997). Comparing ringing loads from experiments with cylinders of different diametersan empirical study. In: *Proceedings of the 8th International Behaviour of Offshore Structures, BOSS 97 Conference.*

Sussman, M., Smereka, P. and Osher, S. (1994). A level set approach for computing solutions to incompressible two-phase flow. *Journal of Computational Physics*, **114**, 146–159.

Welch, S., Levi, C., Fontaine, E. and Tulin, M. (1999). Experimental study of the ringing response of a vertical cylinder in breaking wave groups. *International Journal of Offshore and Polar Engineering*, **9**(04).

Wilcox, D.C. (1994). *Turbulence modeling for CFD.* DCW Industries Inc., La Canada, California.